Parasitology Research (2019) 118:2053–2063
https://doi.org/10.1007/s00436-019-06364-0

PROTOZOOLOGY - ORIGINAL PAPER

Inhibitory activity of chitosan nanoparticles against *Cryptosporidium parvum* oocysts

Shahira A. Ahmed[1] · Heba S. El-Mahallawy[2] · Panagiotis Karanis[3]

Received: 1 February 2019 / Accepted: 24 May 2019 / Published online: 11 June 2019

Abstract

Cryptosporidium is a ubiquitous harsh protozoan parasite that resists many disinfectants. It remains viable and infective for a long time in water and food causing global outbreaks. Chitosan (the deacetylated chitin molecule) was used in its nanosuspension form to evaluate its effect against *Cryptosporidium parvum.* The experiments were performed in vitro in serial concentrations and confirmed in mice in vivo infectivity assay. Chitosan nanoparticles (Cs NPs) were toxic to *Cryptosporidium* oocysts. The effect appeared to decrease the number of *Cryptosporidium* oocysts and altered their content. The destruction rate of oocysts was dependent on the dose of chitosan and the time of exposure ($P < 0.05$). Higher doses of Cs NPs over a prolonged period exhibited a significantly higher destruction rate. Using staining and light microscopy, remarkable destructive changes were observed in the oocysts' morphology. The minimal lethal dose for > 90% of oocysts was 3000 μg/ml, no mice infections in vivo were observed. The results in this study elucidate Cs NPs as an effective anti-cryptosporidial agent.

Keywords *Cryptosporidium* · Chitosan · In vitro · Nanoparticles · Bioassay · Activity

Introduction

Cryptosporidium is able to infect the gastrointestinal tract of humans and most vertebrate animals. It was the major responsible pathogen for 905 waterborne and 25 foodborne outbreaks worldwide (Karanis et al. 2007; Baldursson and Karanis 2011; Efstratiou et al. 2017; Ahmed and Karanis 2018a; Ryan et al. 2018). Currently, there are 41 species with more than 60 genotypes for *Cryptosporidium* (Holubová et al. 2019) reported. Among them, *Cryptosporidium hominis* (*C. hominis*) and *Cryptosporidium parvum* (*C. parvum*) are the most commonly pathogenic species in humans. *C. hominis* can be transmitted directly or indirectly from person to person, whereas *C. parvum* has a zoonotic transmission and bovine animals are the main reservoir hosts (Plutzer and Karanis 2009; Cacciò and Chalmers 2016; Koehler et al. 2017). *Cryptosporidium* is reported to be second after rotavirus, cause of moderate to severe diarrhoea during the first 2 years of life (Kotloff et al. 2012). The species *C. hominis* and *C. parvum* are responsible for nearly a million deaths in humans each year (Villanueva 2017). *C. parvum* was reported as the cause of many economic losses in livestock due to its high mortality rate, loss of production and treatment costs (Shahiduzzaman and Daugschies 2012).

In developing countries, *Cryptosporidium* is one of the most prevalent waterborne protozoa (WBP) (Efstratiou et al. 2017). It is considered the fourth major contributor to diarrhoea in seven regions of Sub-Saharan Africa and Asia (Checkley et al. 2015). Egypt took the lead to document nearly 1/3 (36/120) of WBP reports in Africa (Ahmed et al. 2018) with probably an abundant presence of *Cryptosporidium* in various Egyptian water resources. Robustness of *Cryptosporidium* oocysts, their small size, the low infectious dose, resistance to the most common water disinfectants, long-term viability (6–12 months) and multiple exposure routes (Omarova et al. 2018) make *Cryptosporidium* a very difficult pathogen to control it.

Shahira A. Ahmed and Heba S. El-Mahallawy contributed equally to this work.

Section Editor: Julia Walochnik

✉ Shahira A. Ahmed
shahira_ahmed@med.suez.edu.eg

[1] Department of Parasitology, Faculty of Medicine, Suez Canal University, Ismailia 41522, Egypt

[2] Department of Animal Hygiene, Zoonoses and Animal Behaviour and Management, Faculty of Veterinary Medicine, Suez Canal University, Ismailia 41522, Egypt

[3] University of Cologne, Medical Faculty and University Hospital, 50937 Cologne, Germany

Egypt, as many African countries, faces the huge challenges in its water treatment to make it suitable for human consumption. Chlorine is still currently being used in high doses as the main disinfectant for water and *Cryptosporidium* oocysts are known to be highly chlorine tolerant (CDC 2016). Many compounds have been used in vitro to treat contaminated drinking water against *Cryptosporidium* and have been proven effective, but the safety margin for many of them is still uncertain (Abebe et al. 2015). In developing countries, the population culture relies on the use of low-cost natural remedies. Cost and safety are main factors that must be considered during the selection and use of any putative anti-cryptosporidial agent.

Chitosan is a non-toxic polysaccharide derived from shrimp and crabs with natural chitin alkaline deacetylation (Yong et al. 2015). The use of chitosan has been extended to various fields due to its multiple advantages (agriculture, food packing, cosmetic industries, water treatment and pharmaceutical) (Kong et al. 2010; Muzzarelli et al. 2012). Chitosan intrinsic factors (positive charge density, chelating capacity, physical state, etc.) are particularly responsible for its antimicrobial activities (Kong et al. 2010). It is known to be low in cost and non-toxic that ensures its suitable applicability in developing countries.

Several investigations studied the chitosan activity against microbes and relay to the variety of applications. Forms of nanoparticle have been reported more efficiently than the original compound itself (Jain 2008). Recently, chitosan nanoparticles (Cs NPs) have been proven to be an effective anti-fungal, anti-bacterial and anti-protozoal agent. As an antimicrobial drug, Cs NPs were mostly used as a carrier for drugs delivery (Wang et al. 2011; Jamil et al. 2016; Nehra et al. 2018; Lee et al. 2018). Cs NPs showed also a significant effect on many public health protozoa, successfully used as anti-*Trypanosoma*, anti-*Toxoplasma*, anti-*Leishmania* and anti-*Plasmodium*, in vitro and in vivo (Tripathy et al. 2012; Chaubey and Mishra 2014; Unciti-Broceta et al. 2015; Teimouri et al. 2018).

Several types of NPs (gold and silver based) were used as anti-cryptosporidial agents, but toxic side effects during their use have been reported (Cameron et al. 2016; Benelli 2018). In addition, gold and silver NPs are more expensive for nanotech companies than using the Cs NPs. The inactivation of *Cryptosporidium* oocysts is necessary for adequate control of infection for humans and animals. The unique characteristics of *Cryptosporidium* oocysts and the recognized increased presence in African countries have made it a good model for Cs NPs trilling.

The objective in this study was to investigate the anti-cryptosporidial activity of Cs NPs against *C. parvum* (a) in vitro trials and (b) to proof the infectivity of the Cs NPs-treated oocysts in in vivo bioassays using mice.

Methodology

The protocols for sample collection, the laboratory animal housing and inoculations were reviewed and approved by the Scientific Research Committee and Bioethics Board of Suez Canal University, Faculty of Medicine, Ismailia, Egypt.

Oocysts source

Cryptosporidium oocysts were obtained from six neonatal calves that were suffering from watery diarrhoea on a farm with a known history of recent cryptosporidiosis, located in El-Salhya El Gadeda, Ismailia, Egypt. The farm was specifically selected by a veterinary doctor, who had previously worked on the farm in the feeding section for the neonatal calves. Ten faecal samples were examined in the laboratory using the modified technique of Ziehl-Neelsen (MZN) (Henriksen and Pohlenz 1981). Six samples contained heavy cryptosporidial infection (≥ 4–5 oocysts/field) and were selected for further processing in the experiment. About 1 ml of the watery faecal specimens was transferred directly into 1.5-ml Eppendorf tubes and kept for further molecular identification and confirmation at − 20 °C. The remaining faecal samples were then filtered using four layers of gauze and preserved in potassium dichromate (1:4, *v*/*v*) for further oocysts purification at 4 °C. The preserved oocysts were kept 3 days before proceeding to the purification step.

Collection and purification of oocysts

Sedimentation with ethyl acetate (formalin was replaced by PBS), followed by discontinuous gradient sucrose flotation was used to concentrate and purify the oocysts from faecal samples of the calves (Castro-Hermida et al. 2004; Kourenti and Karanis 2006).

The faecal specimens preserved in potassium dichromate were washed twice in 15-ml tubes with phosphate buffered saline (PBS) with a pH of 7.2). Ethyl acetate was added over the faecal-PBS suspension to form the top 3 ml in each tube. The tubes were sealed tightly and shaken vigorously for 20 seconds (s); they were then centrifuged for 10 minutes (min) at 2100 g. The top lipid layer plug was then removed with a wooden stick after loosening. Then, supernatant was decanted and the remaining sediment was successively washed three times with PBS. The sediments were re-suspended in 3 ml of PBS and overlaid on a discontinuous gradient sucrose. In brief, modified Sheather's sugar (El-Nasr Co. for Intermediate Chemicals, Egypt, www.nasrchemicals.com) stock solution (500 g sucrose +320 ml water, no phenol and no tween) was diluted with PBS to form two different specific gradient gravity solutions, solution A (1:2 *v*/*v*, specific gravity 1.11) and solution B (1:4, specific gravity 1.07). A total of 5 ml of solution A was poured into a 15-ml conical tube, with gentle addition of 5 ml of

solution B. The oocysts' suspension previously prepared (3 ml) was then gently overlaid on the gradient. The gradient tubes were centrifuged for 30 min at 1200 g (Universal Centrifuge, PLC-012E). The second layer was then separated from the top and washed with saline consecutively, followed by a final PBS wash. Sediments (about 1 ml/each tube) were examined for the presence of *Cryptosporidium* oocysts in both wet mount (WM) and MZN stain. The purified oocysts were preserved for subsequent experiments in 2.5% of potassium dichromate 1:4 *v*/*v* at 4 °C.

Molecular identification of *Cryptosporidium* oocysts

Molecular confirmation was performed to identify the species/genotypes of *Cryptosporidium*. The frozen faecal specimens were thawed with cold PBS and filtered through double gauze layers. Consecutive washing with PBS was performed and centrifugation was followed. About 200 μl of the sediment obtained was used to extract DNA using the Qiagen DNA stool mini kit (50, product of Germany) as directed by the manufacturer. As a small modification to the Qiagen protocol, the water bath temperature was raised to 90 °C. The final DNA aliquot of 100 μl was kept for PCR amplification at − 20 °C.

The nested PCR system was used to amplify 18S rDNA gene of *C. parvum* according to Bialek et al. (2002). The outer primer set was CPr I (5-AAA CCC CTT TAC AAG TAT CAA TTG GA-3) and CPr II (5-TTC CTATGT CTG GAC CTG GTG AGT T-3), while the inner primer set was CPr III (5-TGC TTA AAGCAG GCA TAT GCC TTG AA-3) and CPr IV (5-AAC CTC CAA TCT CTA GTT GGC ATA GT-3). The primary PCR reaction mixture was carried out in a total volume of 25 μl (5 μl template DNA, 12.5 μl master mix (Applied Biotechnology Co. Ltd., Egypt) and 20 pm from each of the outer primers). The secondary PCR reaction mixture was typical of the primary PCR, with the exception of using 5 μl of the first amplification product as a template and 25 pm of each inner primer. Control positive and control negative were also included in the reaction. The amplification was performed in a thermocycler (techneTC-312) at 94 °C for 5 min for the initial heating, following 35 cycles of 94 °C for 30 s, 55 °C for 30 s, 72 °C for 45 s, and the final extension at 72 °C for 5 min. The amplified products were visualized after electrophoresis with a 1% agarose gel stained with ethidium bromide using a UV transilluminator.

Preparation of Cs NPs

Cs NPs were purchased from Nanotech for Photo Electronics Company, Egypt (http://www.nanotecheg.com/), prepared and photographed according to their manual. The white Cs NPs suspension was prepared based on the ionotropic gelation of chitosan with tripolyphosphate (TPP) anions (Calvo et al. 1997). Chitosan bulk was dissolved in acetic aqueous solutions at a concentration of 3 mg/ml. Chitosan and TPP were dissolved in purified water in order to obtain solutions of 1 mg/ml (*w*/*v*) and 0.42–0.69 mg/ml (*w*/*v*), respectively, to reach the final theoretical Cs/TPP ratios of 3.6:1–6:1 (*w*/*w*).

The incorporation of 1.2 ml of the TPP solution into 3 ml of the chitosan solution was performed under mild magnetic stirring at room temperature to form the final NPs. NPs were centrifuged (8000*g*/30 min at 15 °C) and the re-suspension volumes were adapted accordingly (Fernández-Urrusuno et al. 1999; Grenha et al. 2005). The morphological examination of Cs NPs was conducted by a high-resolution transmission electron microscopy JEOL JEM-2100 at an accelerating voltage of 200 KV. The measurements of the size of the nanoparticles and zeta potential were performed on freshly prepared samples by using photon correlation spectroscopy and laser Doppler with an average size of 20 ± 5 nm.

In vitro exposure of *Cryptosporidium* oocysts to Cs NPs

Neubauer haemocytometer was used in the previously prepared suspension (the "collection and purification of oocysts" section) to determine the concentration count of the cryptosporidial oocysts. The mean of the four haemocytometer counts of the stock suspension with the dilution factor was calculated after several washes with PBS (to get rid of potassium dichromate) (Finch et al. 1993). A 10-μl aliquot of oocyst suspension was mixed and pipetted between the counting chambers and the haemocytometer cover slide. Oocysts were enumerated under × 40 objective using a phase contrast microscope. Oocysts with a final concentration of (1×10^6/ml) were incubated in sterile PBS (pH 7.4) and an antibiotic (Pen/Strep/Amphotericin B (100×), BioWhittaker®, Lonza) suspension (10,000 U Pen/ml, 10,000 μg Strep/ml, 25 μg Amphotericin B/ml) at room temperature. Various concentrations of Cs NPs (500, 1500, 3000, 5000, 7000 μg/ml) were added to the calculated oocysts' suspension to form a total volume of 1 ml. For comparison with chitosan nanoparticle-treated oocysts (CsTO), a control of untreated oocysts (CUO) was prepared (*Cryptosporidium* oocysts, PBS, antibiotic). CsTO was evaluated after 2, 24 and 72 hours (h) of incubation with Cs NPs for changes in count, viability and morphology (shape and size of the oocysts). Results were compared with CUO for each time period and the changes were determined.

Count distress was determined on Neubauer haemocytometer in a 10 μl (taken from a mixture of 10 μl of CsTO with 10 μl Trypan blue (TB) dye 0.4%) as previously stated. The number of oocysts/μl was then calculated as previously described (Kao and Ungar 1994). The viable *Cryptosporidium* oocysts (unstained with yellow lustre) in the two champers of the haemocytometer were counted

against the non-viable oocysts (stained with blue colour of TB) at × 40. The lethal dose was calculated by a destruction rate equation of (A−B/A) × 100, whereas *A* = mean number of intact oocysts in the control tube, while *B* = mean number of intact oocysts in the chitosan-treated tubes (Hussein et al. 2018). The minimum lethal concentration (MLC) was estimated according to the lowest Cs NPs concentration resulting in a total absence of the visible cryptosporidial endogenous components (Armson et al. 1999).

Changes in the morphological shape of CsTO were examined using light microscopy examination of WM, TB and MZN. Cs NPs were also examined using the same manoeuvre to determine their shape and staining affinity for easy differentiation from the oocysts tested. Changes in the morphological size were estimated using the Olympus bright field × 100 oil immersion lens with an ocular micrometre (carefully calibrated from a stage micrometre). The in vitro exposure assay was performed three times for each concentration of Cs NPs and for each sample. The various Cs NPs concentrations were selected based on previous observations (Ahmed, unpublished data).

In vivo infectivity assays using mice to confirm the in vitro activity of Cs NPs

Nine-week-old, male SPF Swiss Albino mice with an average weight of 24–32 g were purchased. Upon arrival, the mice were randomly divided into six groups, and they were grouped followed the experimental design of Karanis and Schoenen (2001), each with three animals (group I: negative control, group II: CUO, groups III–VI: CsTO) (Table 2). All mice were kept separately under standard conditions of the animal house of Faculty of Medicine, Suez Canal University. While the mice were purchased as pathogen free, its faeces were examined by WM and MZN for three consecutive days (Ma and Soave 1983; Ungar et al. 1990). Four mice were excluded from the experiment due to the contamination with *Eimeria* spp. and *Hymenolepis diminuta* and replaced by others freely examined. After confirming their pathogen-free status, the mice received 500 μl CsTO suspension inoculums with a pre-counted viable oocysts number using a haemocytometer/TB (Table 2) (Karanis and Schoenen 2001). All of the mice were gavaged in the same time with the estimated inoculums. Fresh stool samples were collected from each mouse by applying gentle pressure on their abdomens. Oocysts shedding in mice faecal samples were investigated at (day 3, 5, 6, 7 and 10) post-inoculation by using MZN stain after purification. All of the mice were sacrificed (by cervical dislocation) on the 10th day post-inoculation. The evidence of infection for each group was determined by plus (positive) or minus (negative) scores following the microscopic observations of *Cryptosporidium* oocysts as described by Korich et al. (2000).

Statistical analysis

The statistical significance of the variations between different concentrations of Cs NPs and the *Cryptosporidium* oocysts at different time periods was determined using a two-way analysis of variance (ANOVA). The ANOVA test is ideal to test the statistical significance of the variations observed between means of data. In this study, *p*-values of ≤ 0.05 were considered significant. All the analyses were done with the IBM SPSS Statistics V23.0 (IBM Corp., Armonk, NY, USA).

Results

Molecular identification of the oocysts used

With the use of nested PCR system specific for *C. parvum*, the *Cryptosporidium* species from the investigated samples has been identified. All the calves' faecal samples were infected with *C. parvum*. The amplified product of 285 bp was successfully electrophoresed from the six samples (Fig. 1).

Morphology of Cs NPs

The size and distribution of Cs NPs were examined by WM and TB techniques. TB stained Cs NPs with blue colour, clearly differentiating them from the unstained *Cryptosporidium* oocysts. With the use of MZN, Cs NPs appeared less structured and unstained in comparison with rose-stained oocysts.

In vitro exposure of oocysts to Cs NPs

Anti-cryptosporidial activity of Cs NPs (count stress)

The in vitro anti-cryptosporidial inhibitory activity of different concentrations of Cs NPs is summarized and presented in Fig. 2. Different concentrations of Cs NPs resulted in 'visible stress' on the overall count of *Cryptosporidium* oocysts ($P < 0.05$). The percentage of oocysts reduction was calculated using the equation of destruction rate. The highest oocysts destruction mean was observed after 72 h at a concentration of 5000 μg/ml; however, a full destruction rate (99.8%) was observed after 72 h at a concentration of 7000 μg/ml. The statistics also showed a significant difference between the tested concentrations of Cs NPs over various time intervals throughout the experiment ($P < 0.05$).

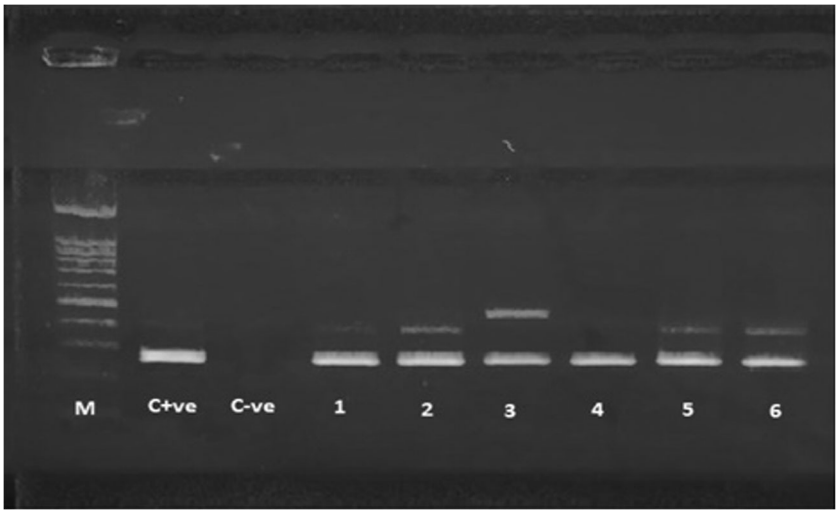

Fig. 1 Nested PCR of six faecal samples from calves. M, 100 bp DNA ladder (Applied Biotechnology Co. Ltd., Egypt). Lane 1, positive control; lane 2, negative control; lane 3–8, samples used as source for *Cryptosporidium* oocysts

Changes in oocysts morphology due to Cs NPs toxicity

Normally, *Cryptosporidium* oocysts appeared bright in colour and measured 4–6 μm, with a central globule, 1– 4 sporozoites and eccentric dark granules. Cs NPs had remarkable toxic effects on the oocysts, affecting their size and morphology, ending with destruction of oocysts (Table 1, Fig. 3). It was noted that changes could be tracked in the following stages:

Stage 1: Oocysts appeared to be similar to their normal size, they lost their bright colour, turning grey (TB) and filled with undifferentiated substances in their inner content.

Stage 2: Oocysts were enlarged and/or swollen with an intact wall, coloured grey and their internal content was filled with a large vacuole or multiple vacuoles.

Stage 3: Oocysts were enlarged with corrugated wall, and their content appeared as granules, being completely destroyed.

Stage 4: Oocysts were cracked and their structure had shrunk, their wall was shredded and their content expulsion was either seen attached to the wall or distributed near the oocysts that were damaged.

In vivo infectivity assay to confirm viability and infectivity of the oocysts

Although the results of the in vitro assay clearly indicated that three concentrations (3000, 5000, 7000 μg/ml) of Cs NPs were able to completely destroy > 90% of the visible endogenous components of *Cryptosporidium* oocysts, a question remains unanswered, whether the remaining intact oocysts are viable and capable of causing infection or not. The in vivo assay details and results are presented in Table 2. Infectivity was noted in 2/6 groups (groups II and III), whereas groups IV, V and VI showed no infectivity. Group I (the negative control) showed negativity throughout the experiment.

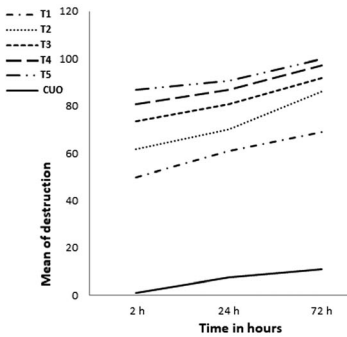

*Concentrations of Cs NPs	Time (hours)		
	2 hours	24 hours	72 hours
	Mean destruction rate (%) ± (SD)	Mean destruction rate (%) ± (SD)	Mean destruction rate (%) ± (SD)
T1=500μg/ml	49.9 ± (0.9)	60.6 ± (0.7)	68.88 ± (2.9)
T2=1500μg/ml	61.8 ± (1.2)	70 ± (1.8)	86 ± (0.7)
T3=3000μg/ml	73.6 ± (0.5)	80.8 ± (1.7)	91.9 ± (0.9)
T4=5000μg/ml	80.6 ± (0.3)	87 ± (0.8)	97.3 ± (1)
T5=7000μg/ml	88 ± (1)	90.5 ± (1.3)	99.87 ± (0.2)

Fig. 2 Count distress of oocysts by mean of destruction rate in different time of exposure with various concentrations of Cs NPs (right table) compared with CUO: control untreated oocysts (left figure). Values are given as the mean ± SD of triple experiments. *Destruction rates in different concentrations at different time intervals were statistically significant *P* value = 0.00

Table 1 Descriptive changes in morphology and size of CsTO against CUO using WM, TB and MZN techniques

Oocysts	Technique	Shape	Content	Colour	Size	
					Range (μm)	Average(μm)
CUO	WM	Rounded	Presence of (1–3) sporozoites/oocysts "longitudinal/-vertical according to its captured photographed position", residuum of small one/several eccentric dark granules. Central or membrane bound globule. White hallo around each oocyst.	Refractile bright structure	4–5	4.5
	TB	Rounded	Oocysts resembled WM appearance.	Intense bright colour against background of TB	4–5	4.5
	MZN	Rounded-elliptical	Stained oocysts wall with internal sporozoites. Discernible sporozoites with remarkable crescent/galactic shape. Presence of unstained translucent globule.	Colour varied from light rose to rose red against background of malachite green	4–5	4.5
CsTO	WM	Rounded-semi rounded, swollen, distorted	It has been difficult to discriminate stages of destroyed oocysts under LM by WM examination; however, some oocysts appeared same size to normal and others were swollen with white halo around the oocysts. Only intact wall oocysts could be well recognized with internal multiple vacuoles. Late stage, absence of sporozoite architecture was remarkable. Changes were recognized hardly at × 100.	Structure lost its bright refractile property and tend to be light grey colour	5–8	6.5
	TB	Rounded-semi rounded-swollen-distorted	TB was an excellent stain to show remarkable changes in CsTO. Oocysts were same size to normal and others appeared with marked enlargement. Intact oocyst's wall integrity was frequently noticed, whereas few torn oocyst's wall was seen clearly with expelled content. Changes were easily recognized at × 40 and confirmed with × 100.	Non-viable grey colour of content and grey colour of oocysts wall against blue background of Trypan blue	5.5–8.5	7
	MZN	Rounded-half circular-no identified shape	MZN was a very good technique to demonstrate changes in treated oocysts particularly the torn ones. Most oocysts seen enlarged with cracked wall. In intact oocysts, the sporozoite architectures were completely destroyed either in the form of vacuoles or small granules. In cracked oocysts, the sporozoites usually expelled out, either attached to the oocysts wall or totally expelled nearby the oocysts. Changes were easily recognized at × 100	Colour of intact oocysts wall varied between pink to rose red. However, its undifferentiated content took rosy colour. Colour of cracked oocysts wall varied between translucent to bright pink. However, its content "if have" took the rosy red colour.	5.5–8.5	7

CUO, control untreated oocysts; *CsTO*, chitosan nanoparticle-treated oocysts; *WM*, wet mount; *TB*, trypan blue; *MZN*, modified Ziehl-Neelsen; *μm*: micrometre

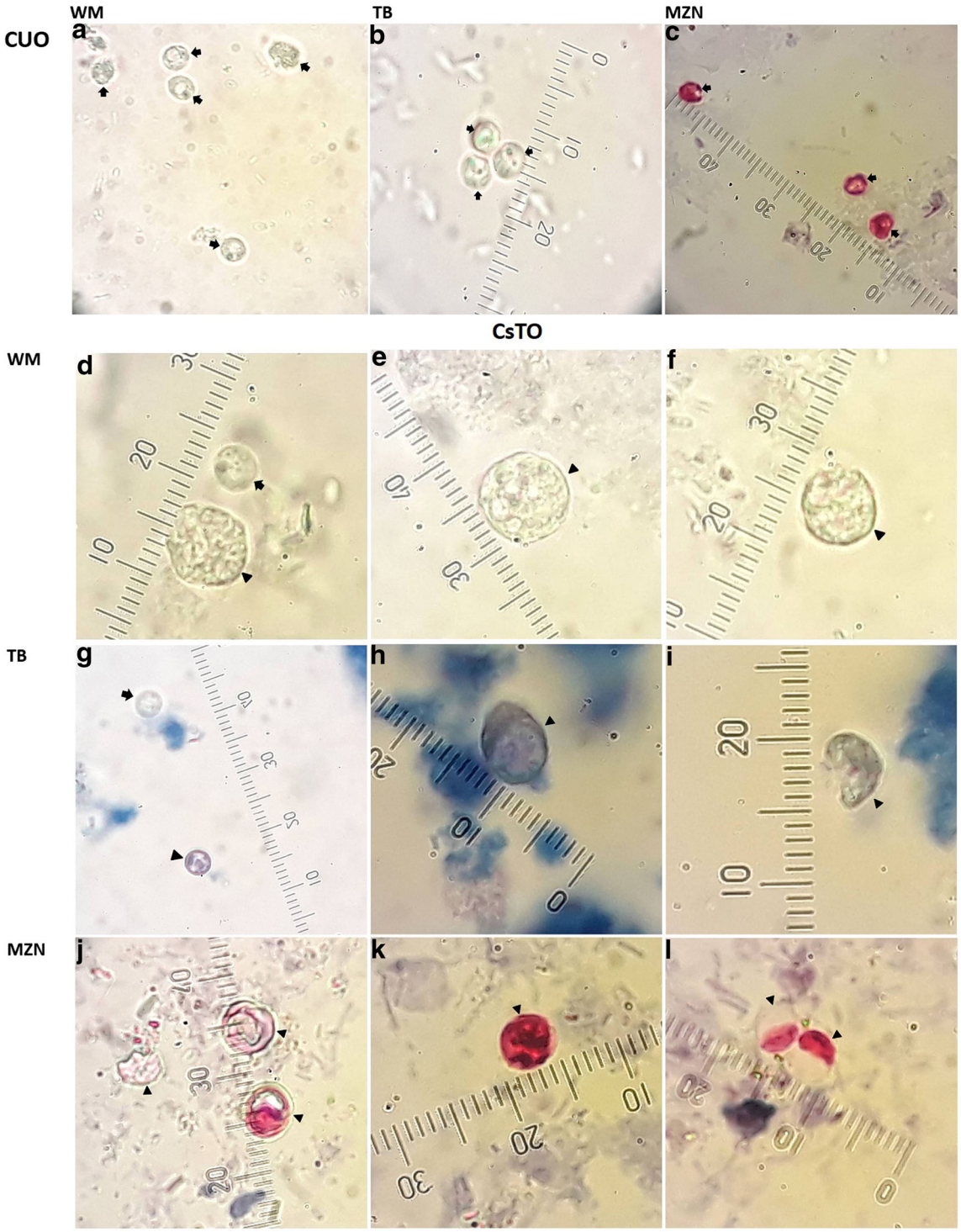

Fig. 3 Visible effect of Cs NPs on morphology of CsTO against CUO using WM, TB and MZN (three pictures/each). Panels **a**–**c** are related to CUO, horizontal arrangement of WM (**a**), TB (**b**), MZN (**c**). Panels **d**–**l** are related to CsTO, vertical arrangement of WM (**d**–**f**), TB (**g**–**i**), MZN (**j**–**l**). Normal shape and size *Cryptosporidium* oocysts were pointed out by arrow, whereas treated oocysts were indicated by arrow head. Pictures explain the serial changes in morphology of oocysts and are not related to different concentrations of Cs NPs

Discussion

Nanotechnology has recently been emerged with its proven anti-microbial activity and chitosan is known to be a biocompatible system with bacteriostatic properties that increase its use in the pharmaceutical field (Kong et al. 2010; Katas et al. 2013). In developing countries, cost effectiveness is an important modulator prior to any control programme. In

Table 2 Design and results of in vivo assay

Groups	No. of mice/group	Mean inoculum/ mouse	Inoculation time line[a]	Number of positive mice/no. of inoculated mice	Starting day of shedding
Group I	3	No inoculum	Inoculated with PBS	0/3	No shedding
Group II	3	89×10^4	Inoculated[b] with 500 μl CUO/animal	3/3	Day 3
Group III	3	48×10^4	Inoculated[b] with 500 μl from 500 μg/ml CsTO/animal	2/3	Day 7
Group IV	3	9×10^4	Inoculated[b] with 500 μl from 3000 μg/ml CsTO/animal	0/3	No shedding
Group V	3	2.5×10^4	Inoculated[b] with 500 μl from 5000 μg/ml CsTO/animal	0/3	No shedding
Group VI	3	0.5×10^4	Inoculated[b] with 500 μl from 7000 μg/ml CsTO/animal	0/3	No shedding

[a] Infectivity assay started at day 0 and ended at day 10 post-infection. [b] Mice were inoculated orally by gastric gavage with 500 μl (oocysts in PBS). Experiments were designed based on Karanis and Schoenen (2001)

Egypt, people prefer to use natural products for treatment instead of synthetic chemical drugs, particularly in the rural areas. The fact that natural products are cost-effective and did not have side effects made them favourable. Ionotropic gelation is a method commonly used for preparation of nanoparticles and it does not require introduction of chemical groups into the chitosan molecules (Vaezifar et al. 2013). Cs NPs have been previously used in different studies because of their cost effectiveness, non-toxic properties, stability, simple preparation methodology and biodegradability (Nagpal et al. 2010; Potdar and Shetti 2016). In Egypt, Cs NPs have recently been used as anti-bacterial (Shetta et al. 2019; Marei et al. 2019) and anti-protozoal agents (anti-*Giardia* and anti-*Toxoplasma*) (Said et al. 2012; Gaafar et al. 2014; Etewa et al. 2018) with effective results.

Since *Cryptosporidium* oocysts are highly stable and maintain viability in water for up to 12 months, they can cause waterborne epidemics even from purified drinking water (Omarova et al. 2018). Therefore, *Cryptosporidium* would be a unique pathogen to observe its visible interaction with Cs NPs. In this study, we investigated the toxic effect of Cs NPs against *Cryptosporidium* oocysts in vitro and had confirmed the results with infectivity assay in vivo using mice. To the authors' best knowledge, this is the first report to test the effects of serial concentrations of Cs NPs on the *Cryptosporidium* protozoan parasite using simple techniques. Fortunately, infected calves shed large numbers of *Cryptosporidium* in their diarrhoea and they were easily accessible at farms. It was therefore easy to collect samples and purify enough amount of oocysts to perform the experiments. *C. parvum* has been reported to be the dominant species in pre-weaned calves (Gong et al. 2017). Moreover, *C. parvum* species are capable of infecting both humans and animals; therefore, the results of any experiment involving this protozoan would reflect its applicability to both hosts.

Our data revealed dose-dependent toxic activity of Cs NPs, showed a damage effect to the *Cryptosporidium* count and altered its content. Over the range of concentration doses, Cs NPs triggered a destructive process of oocysts at 500 μg/ml, while 3000 μg/ml was the minimal concentration dose that killed > 90% of oocysts and continued their non-infectivity in mice. The destructive mechanism of low doses of Cs NPs might be due to its small size and excellent film forming ability. The small size of the nanoforms usually expose large surface area to volume ratio (Bell et al. 2014) and increase the in vitro efficacy by increasing the dissolution and bioavailability. The destructive effect could therefore potentially increase the electrostatic interaction between Cs NPs and oocysts. Such interaction would change the integrity and permeability of the oocysts wall leading to their destruction.

It was noted that the destruction rate of oocysts was time dependent and it increased over an extended period of time (72 h) with the contact with Cs NPs. After 2 h, the destruction process of oocysts was initiated, while Cs NPs were noted to surround oocysts. Oocysts started to lose their refractile colour and turned grey, but they maintained their normal size. After 24 h, oocysts started to swell, inflate and change their outer spherical shape with degradation of their contents. A quantity of oocysts has been disrupted at this point. After 72 h, almost none of the viable oocysts were detectable in the field (7000 μg|ml). Probably, if the oocysts had remained with Cs NPs for a longer time period (f.e. 7 days), the lowest concentration of 500 μg|ml would destroy all of the oocysts present in the field based on a previous pilot study (data unpublished).

In other studies, the effect of NPs on *E. coli*, *S. cholera suis*, *S. typhimurium* and *S. aureus* was evaluated over short periods of time (30–180 min) and showed good outcomes (Qi et al. 2004). The difference in the biological properties of the microorganisms could explain in part the dissimilarity of data. *Cryptosporidium* is a ubiquitous parasite with a hard oocyst wall; a reason why it may require a longer contact time with Cs NPs to achieve full toxicity. Similarly, *Cyclospora cayetanensis* (with an oocyst wall) required a longer time with magnesium NPs in order to be destroyed (Hussein et al. 2018). Therefore, prolonged contact time with NPs is preferable when dealing with harsh parasites like *Cryptosporidium*.

Recent research has experienced the use of expensive approaches (electron and hyperspectral microscopes) to demonstrate effect of drugs on parasites (Chaubey and Mishra 2014; Gaafar et al. 2014; Cameron et al. 2016). However, light microscope remains the simplest and cheapest method for diagnostic and observational purposes when using the correct stain (Ahmed and Karanis 2018b). It also suits the common diagnostic strategies in developing countries. In the present study, changes in the morphology of *Cryptosporidium* oocysts due to the destructive effect of Cs NPs are clearly demonstrated by light microscope using WM, TB and MZN.

The wet mount examination is a simple, fast, time-saving and cost-effective technique but the diagnosis of *Cryptosporidium* oocysts requires a well-experienced individual. Oocysts' WM examination is easier if the sample contains purified, untreated oocysts, but the diagnosis is more difficult if oocysts are exposed to Cs NPs. This led to failure to recognize some changes in oocysts morphology by WM after exposure to Cs NPs. Cs NPs formed a hazy background similar in colour to the *Cryptosporidium* oocysts, resulting in extremely difficult oocysts differentiation, particularly at higher concentrations (Fig. 3d–f).

On the contrary, TB was an excellent staining technique, allowing for easy and clear visualization of refractile *Cryptosporidium* against a blue stained background of Cs NPs. Obviously, it was easy to differentiate between viable and non-viable oocysts. While the viable oocysts have a refractile appearance, the non-viable oocysts stained grey in colour against a shiny blue background. The extra benefit of TB was its ability to differentiate all the previous details on a lower magnification (× 40) (Fig. 3g–i).

MZN staining was also a good technique; however, variation in the stained colours of the treated oocysts should be considered. Initiation of colour variation could return to the cracked oocysts wall. The oocysts wall could be responsible for maintaining the *Cryptosporidium's* acid-fast property. Once an opening has been formed in the oocyst wall, it cannot be stained normally anymore. Consequently, after being stained, the oocysts wall varies in colour between translucent, pink, light rose and deep rose based on cracking of oocysts' wall. Their contents, however, still retained their rose colour either inside or outside the oocysts' cells (Fig. 3j–l).

Nanoforms are known to evoke cellular stress responses not only at low doses, but also over long periods of exposure (Bell et al. 2014). It was suggested that chitosan anti-microbial activity resulted from a series of reactions, rather than the cause of the reactions themselves (Kong et al. 2010). The observed destruction of oocysts by Cs NPs (Fig. 3d–l) might be due to its large surface area. This large surface area of Cs NPs has the ability to ease its adsorption to the surface of oocysts wall causing its disruption through formation of pits or dimples. An interaction could result in leakage of the components of the oocysts. This could explain the oocysts' enlargement and formation of multiple small and/or large vacuoles. The vacuoles fill the space inside the oocysts, transforming its entire components into small undifferentiated granules. As the swelling increases, the oocyst wall is pressurised from the inside. The oocysts wall is then cracked under pressure and all of the oocyst contents were expelled.

Similar scenarios concerning the effect of Cs NPs as antibacterial or anti-protozoal agents have been mentioned in several articles (Qi et al. 2004; Xing et al. 2009; Gaafar et al. 2014). Other types of NPs also displayed close action (Cameron et al. 2016; Hussein et al. 2018). Another explanation is that chitosan and its derivatives possess a positive surface charge (Mohammed et al. 2017). The wall of *Cryptosporidium* oocysts has negative charge (Searcy et al. 2006). Such properties could increase the ability of both chitosan and oocysts to stick together and thus increase the chitosan anti-cryptosporidial activity. However, chitosan's exact mechanism of action still remains unknown; a topic which would be favourable for further research.

The animal model remains the gold standard of oocysts viability assessment methods (Robertson and Gjerde 2007). CsTO were fed to mice to determine whether the in vitro effect of Cs NPs could achieve any infectivity in vivo or not. The neonatal animal model is considered highly susceptible for the *C. parvum* infection (Mammeri et al. 2018); neonatal mice, however, could not be easily obtained for animal model of this experiment, posing as a kind of limitation in this study.

With the minimum lethal concentration (3000 μg/ml) of Cs NPs in vitro, the CsTO did not cause any infection in mice compared with mice fed with CUO infection. Previously conducted in vivo experiments using other protozoan parasite showed similar documented data. Cs NPs have proven their anti-toxoplasmic effects through tachyzoites mortality and increased mice survival compared with the control group (Teimouri et al. 2018). Cs NPs displayed the same effects when combined with other drugs. Spiramycin-loaded Cs NPs decreased the mortality rate of mice infected with *Toxoplasma*. Moreover, on a histopathological basis, it displayed an anti-inflammatory effect by reducing perivascular inflammatory cellular infiltration (Etewa et al. 2018). In malaria, Cs NPs conjugated with chloroquine have been shown to have a therapeutic anti-malarial and antioxidant effect (Tripathy et al. 2012). In this study, Cs NPs were used as a suspension adding an advantage to the use of Cs NPs as powder. Such property increased the anti-cryptosporidial effect of buparvaquone as it remained in the gastrointestinal tract of mice for extended periods of time (Kayser 2001).

The data presented in this study highlights the use of Cs NPs as an effective agent against *C. parvum*. Low doses of this nanoform would be suitable to destroy *Cryptosporidium* oocysts over an extended period of time, particularly in the

form of suspension. The positive effect of using Cs NPs is its simple methodology of application and their high safety level. Although it could not be applied to a wide range and a large amount of water, it could be used to treat water in hospitals to protect immunodeficient patients from life-threatening infection with *Cryptosporidium*. To our knowledge, this is the first study that addresses the effect of Cs NPs on *Cryptosporidium* spp. and further studies are needed to examine its anti-cryptosporidial effect in biological samples.

Compliance with ethical standards

The protocols for sample collection, the laboratory animal housing and inoculations were reviewed and approved by the Scientific Research Committee and Bioethics Board of Suez Canal University, Faculty of Medicine, Ismailia, Egypt.

Conflict of interest The authors declare that they have no conflict of interest.

References

Abebe LS, Su Y-H, Guerrant RL, Swami NS, Smith AS (2015) Point-of-use removal of *Cryptosporidium parvum* from water: Independent effects of disinfection by silver nanoparticles and silver ions and by physical filtration in ceramic porous media. Environ Sci Technol 49: 12958–12967

Ahmed SA, Guerrero Flórez M, Karanis P (2018) The impact of water crises and climate changes on the transmission of protozoan parasites in Africa. Pathog Glob Health 112:281–293

Ahmed SA, Karanis P (2018a) An overview of methods/techniques for the detection of *Cryptosporidium* in food samples. Parasitol Res 117:629–653

Ahmed SA, Karanis P (2018b) Comparison of current methods used to detect *Cryptosporidium* oocysts in stools. Int J Hyg Environ Health 221:743–763

Armson A, Meloni BP, Reynoldson JA, Thompson RCA (1999) Assessment of drugs against *Cryptosporidium parvum* using a simple in vitro screening method. FEMS Microbiol Lett 178:227–233

Baldursson S, Karanis P (2011) Waterborne transmission of protozoan parasites: review of worldwide outbreaks - an update 2004-2010. Water Res 45:6603–6614

Bell IR, Ives JA, Jonas WB (2014) Non-linear effects of nanoparticles: biological variability from hormetic doses, small particle sizes, and dynamic adaptive interactions. Dose-Response 12:202–232

Benelli G (2018) Gold nanoparticles - against parasites and insect vectors. Acta Trop 178:73–80

Bialek R, Binder N, Dietz K, Joachim A, Knobloch J, Zelck UE (2002) Comparison of fluorescence, antigen and PCR assays to detect *Cryptosporidium parvum* in faecal specimens. Diagn Microbiol Infect Dis 43:283–288

Cacciò SM, Chalmers RM (2016) Human cryptosporidiosis in Europe. Clin Microbiol Infect 22:471–480

Calvo P, Remuñán-López C, Vila-Jato J, Alonso MJ (1997) Novel hydrophilic chitosan – polyethylene oxide nanoparticles as protein carriers. J Appl Polym Sci 63:125–132

Cameron P, Gaiser BK, Bhandari B, Bartley PM, Katzer F, Bridle H (2016) Silver nanoparticles decrease the viability of *Cryptosporidium parvum* oocysts. Appl Environ Microbiol 82: 431–437

Castro-Hermida J, Porsi I, Ares-Mazas E, Chartier C (2004) In vitro activity on *Cryptosporidium parvum* oocyst of different drugs with recognized anti-cryptosporidial efficacy. Rev Med Vet (Toulouse) 155:453–456

Centers for Disease Control and Prevention CDC (2016) Hyperchlorination to kill *Cryptosporidium* when chlorine stabilizer 1 is NOT in water. US

Chaubey P, Mishra B (2014) Mannose-conjugated chitosan nanoparticles loaded with rifampicin for the treatment of visceral leishmaniasis. Carbohydr Polym 101:1101–1108

Checkley W, White AC, Jaganath D, Arrowood MJ, Chalmers RM, Chen X-M, Fayer R, Griffiths JK, Guerrant RL, Hedstrom L, Huston CD, Kotloff KL, Kang G, Mead JR, Miller M, Petri WA, Priest JW, Roos DS, Striepen B, Thompson RCA, Ward HD, Van Voorhis WA, Xiao L, Zhu G, Houpt ER (2015) A review of the global burden, novel diagnostics, therapeutics, and vaccine targets for *Cryptosporidium*. Lancet Infect Dis 15:85–94

Efstratiou A, Ongerth JE, Karanis P (2017) Waterborne transmission of protozoan parasites: review of worldwide outbreaks - an update 2011–2016. Water Res 114:14–22

Etewa SE, El-Maaty DAA, Hamza RS, Metwaly AS, Sarhan MH, Abdel-Rahman SA, Fathy GM, El-Shafey MA (2018) Assessment of spiramycin-loaded chitosan nanoparticles treatment on acute and chronic toxoplasmosis in mice. J Parasit Dis 42:102–113

Fernández-Urrusuno R, Calvo P, Remuñán-López C, Vila-Jato JL, Alonso MJ (1999) Enhancement of nasal absorption of insulin using chitosan nanoparticles. Pharm Res 16:1576–1581

Finch GR, Daniels CW, Black EK, Schaefer FW 3rd, Belosevic M (1993) Dose response of *Cryptosporidium parvum* in outbred neonatal CD-1 mice. Pharm Res 16:1576–1581

Gaafar MR, Mady RF, Diab RG, Shalaby TI (2014) Chitosan and silver nanoparticles: promising anti-*Toxoplasma* agents. Exp Parasitol 143:30–38

Grenha A, Seijo B, Remuñán-López C (2005) Microencapsulated chitosan nanoparticles for lung protein delivery. Eur J Pharm Sci 25:427–437

Gong C, Cao XF, Deng L, Li W, Huang X-M, Lan J-C, Xiao Q-C, Zhong ZJ, Feng F, Zhang Y, Wang WB, Guo P, Wu K-Y, Peng GN (2017) Epidemiology of *Cryptosporidium* infection in cattle in China: a review. Parasite 24:1

Henriksen SA, Pohlenz JF (1981) Staining of cryptosporidia by a modified Ziehl-Neelsen technique. Acta Vet Scand 22:594–296

Holubová N, Zikmundová V, Limpouchová Z, Sak B, Konečný R, Hlásková L, Rajský D, Kopacz Z, McEvoy J, Kváč M (2019) *Cryptosporidium proventriculi* sp. n. (Apicomplexa: Cryptosporidiidae) in Psittaciformes birds. Eur J Protistol 69:70–87

Hussein EM, Ahmed SA, Mokhtar AB, Elzagawy SM, Yahi SH, Hussein AM, El-Tantawey F (2018) Antiprotozoal activity of magnesium oxide (MgO) nanoparticles against *Cyclospora cayetanensis* oocysts. Parasitol Int 67:666–674

Jain KK (2008) Nanomedicine: application of nanobiotechnology in medical practice. Med Princ Pract 17:89–101

Jamil B, Habib H, Abbasi S, Nasir H, Rahman A, Rehman A, Bokhari H, Imran M (2016) Cefazolin loaded chitosan nanoparticles to cure multi drug resistant gram-negative pathogens. Carbohydr Polym 136:682–691

Kao TC, Ungar BLP (1994) Comparison of sequential, random, and haemocytometer methods for counting *Cryptosporidium* oocysts. J Parasitol 80:816–819

Karanis P, Kourenti C, Smith H (2007) Water-borne transmission of protozoan parasites: a worldwide review of outbreaks and lessons learnt. J Water Health 5:1–38

Karanis P, Schoenen D (2001) Biological test for the detection of low concentrations of infectious *Cryptosporidium parvum* oocysts in water. Acta Hydrochim Hydrobiol 29:242–245

Katas H, Raja MAG, Lam KL (2013) Development of chitosan nanoparticles as a stable drug delivery system for protein/siRNA. Int J Biomater 2013:146320

Kayser O (2001) A new approach for targeting to *Cryptosporidium parvum* using mucoadhesive nanosuspensions: research and applications. Int J Pharm 214:83–85

Koehler AV, Korhonen PK, Hall RS, Young ND, Wang T, Haydon SR, Gasser RB (2017) Use of a bioinformatic-assisted primer design strategy to establish a new nested PCR-based method for *Cryptosporidium*. Parasit Vectors 10:509

Kong M, Chen XG, Xing K, Park HJ (2010) Antimicrobial properties of chitosan and mode of action: a state of the art review. Int J Food Microbiol 144:51–63

Korich DG, Marshall MM, Smith HV, O'Grady J, Bukhari Z, Fricker CR, Rosen JP, Clancy JL (2000) Inter-laboratory comparison of the CD-1 neonatal mouse logistic dose-response model for *Cryptosporidium parvum* oocysts. J Eukaryot Microbiol 47:294–298

Kotloff KL, Blackwelder WC, Nasrin D, Nataro JP, Farag TH, van Eijk A, Adegbola RA, Alonso PL, Breiman RF, Faruque AS, Saha D, Sow SO, Sur D, Zaidi AK, Biswas K, Panchalingam S, Clemens JD, Cohen D, Glass RI, Mintz ED, Sommerfelt H, Levine MM (2012) The Global Enteric Multicenter Study (GEMS) of diarrheal disease in infants and young children in developing countries: epidemiologic and clinical methods of the case/control study. Clin Infect Dis 55(Suppl 4):S232–S245

Kourenti C, Karanis P (2006) Evaluation and applicability of a purification method coupled with nested PCR for the detection of *Toxoplasma* oocysts in water. Lett Appl Microbiol 43:475–481

Lee EH, Khan I, Oh D-H (2018) Evaluation of the efficacy of nisin-loaded chitosan nanoparticles against foodborne pathogens in orange juice. J Food Sci Technol 55:1127–1133

Ma P, Soave R (1983) Three-step stool examination for cryptosporidiosis in 10 homosexual men with protracted watery diarrhoea. J Infect Dis 147:824–828

Mammeri M, Chevillot A, Thomas M, Polack B, Julien C, Marden JP, Auclair E, Vallée I, Adjou KT (2018) Efficacy of chitosan, a natural polysaccharide, against *Cryptosporidium parvum in vitro* and *in vivo* in neonatal mice. Exp Parasitol 194:1–8

Marei N, Elwahy AHM, Salah TA, El Sherif Y, El-Samie EA (2019) Enhanced antibacterial activity of Egyptian local insects' chitosan-based nanoparticles loaded with ciprofloxacin-HCl. Int J Biol Macromol 126:262–272

Mohammed M, Syeda J, Wasan K, Wasan E (2017) An overview of chitosan nanoparticles and its application in non-parenteral drug delivery. Pharmac 9:E53

Muzzarelli RAA, Boudrant J, Meyer D, Manno N, DeMarchis M, Paoletti MG (2012) Current views on fungal chitin/chitosan, human chitinases, food preservation, glucans, pectins and inulin: a tribute to Henri Braconnot, precursor of the carbohydrate polymers science, on the chitin bicentennial. Carbohydr Polym 87:995–1012

Nagpal K, Singh SK, Mishra DN (2010) Chitosan nanoparticles: a promising system in novel drug delivery. Chem Pharm Bull (Tokyo) 58: 1423–1430

Nehra P, Chauhan R, Garg N, Verma K (2018) Antibacterial and antifungal activity of chitosan coated iron oxide nanoparticles. Br J Biomed Sci 75:13–18

Omarova A, Tussupova K, Berndtsson R, Kalishev M, Sharapatova K (2018) Protozoan parasites in drinking water: a system approach for improved water, sanitation and hygiene in developing countries. Int J Environ Res Public Health 15:495

Plutzer J, Karanis P (2009) Genetic polymorphism in *Cryptosporidium* species: an update. Vet Parasitol 165:187–199

Potdar PD, Shetti AU (2016) Evaluation of anti-metastatic effect of chitosan nanoparticles on oesophageal cancer-associated fibroblasts. J Cancer Metastasis Treat 2:259–267

Qi L, Xu Z, Jiang X, Hu C, Zou X (2004) Preparation and antibacterial activity of chitosan nanoparticles. Carbohydr Res 339:2693–2700

Ryan U, Hijjawi N, Xiao L (2018) Foodborne cryptosporidiosis. Int J Parasitol 48:1–12

Robertson LJ, Gjerde BK (2007) *Cryptosporidium* oocysts: challenging adversaries? Trends Parasitol 23:344–347

Said DE, ElSamad LM, Gohar YM (2012) Validity of silver, chitosan, and curcumin nanoparticles as anti-*Giardia* agents. Parasitol Res 111:545–554

Searcy KE, Packman AI, Atwill ER, Harter T (2006) Capture and retention of *Cryptosporidium parvum* oocysts by *Pseudomonas aeruginosa* biofilms. Appl Environ Microbiol 72:6242–6247

Shahiduzzaman M, Daugschies A (2012) Therapy and prevention of cryptosporidiosis in animals. Vet Parasitol 188:203–214

Shetta A, Kegere J, Mamdouh W (2019) Comparative study of encapsulated peppermint and green tea essential oils in chitosan nanoparticles: encapsulation, thermal stability, in-vitro release, antioxidant and antibacterial activities. Int J Biol Macromol 126:731–742

Teimouri A, Azami SJ, Keshavarz H, Esmaeili F, Alimi R, Mavi SA, Shojaee S (2018) Anti-*Toxoplasma* activity of various molecular weights and concentrations of chitosan nanoparticles on tachyzoites of RH strain. Int J Nanomedicine 13:1341–1351

Tripathy S, Das S, Chakraborty SP, Sahu SK, Pramanik P, Roy S (2012) Synthesis, characterization of chitosan–tripolyphosphate conjugated chloroquine nanoparticle and its *in vivo* anti-malarial efficacy against rodent parasite: a dose and duration dependent approach. Int J Pharm 434:292–305

Unciti-Broceta JD, Arias JL, Maceira J, Soriano M, Ortiz-González M, Hernández-Quero J, Muñóz-Torres M, de Koning HP, Magez S, Garcia-Salcedo JA (2015) Specific cell targeting therapy bypasses drug resistance mechanisms in African trypanosomiasis. PLoS Pathog 11:e1004942

Ungar BL, Burris JA, Quinn CA, Finkelman FD (1990) New mouse models for chronic *Cryptosporidium* infection in immunodeficient hosts. Infect Immun 58:961–969

Vaezifar S, Razavi S, Golozar MA, Karbasi S, Morshed M, Kamali M (2013) Effects of some parameters on particle size distribution of chitosan nanoparticles prepared by ionic gelation method. J Clust Sci 24:891–903

Villanueva MT (2017) Infectious diseases: decrypting *Cryptosporidium*. Nat Rev Drug Discov 16:527–527

Wang J, Zeng ZW, Xiao RZ, Xie T, Zhou GL, Zhan XR, Wang SL (2011) Recent advances of chitosan nanoparticles as drug carriers. Int J Nanomedicine 6:765–774

Xing K, Chen XG, Liu CS, Cha DS, Park HJ (2009) Oleoyl-chitosan nanoparticles inhibits *Escherichia coli* and *Staphylococcus aureus* by damaging the cell membrane and putative binding to extracellular or intracellular targets. Int J Food Microbiol 132:127–133

Yong SK, Shrivastava M, Srivastava P, Kunhikrishnan A, Bolan N (2015) Environmental applications of chitosan and its derivatives. Rev Environ Contam Toxicol 233:1–43